International Journal of Cancer Therapy and Oncology
www.ijcto.org

Evaluation of collapsed cone convolution superposition (CCCS) algorithms in prowess treatment planning system for calculating symmetric and asymmetric field size

Tamer Dawod

Department of Clinical Oncology and Nuclear Medicine, Faculty of Medicine, Mansoura University, Mansoura, Egypt

Received October 21, 2014; Revised February 07, 2015; Accepted March 30, 2015; Published Online April 05, 2015

Technical Report

Abstract

Purpose: This work investigated the accuracy of prowess treatment planning system (TPS) in dose calculation in a homogenous phantom for symmetric and asymmetric field sizes using collapse cone convolution/superposition algorithm (CCCS). **Methods:** The measurements were carried out at source-to-surface distance (SSD) set to 100 cm for 6 and 10 MV photon beams. Data for a full set of measurements for symmetric fields and asymmetric fields, including inplane and crossplane profiles at various depths and percentage depth doses (PDDs) were obtained. **Results:** The results showed that the asymmetric collimation dose lead to significant errors (up to approximately 7%) in dose calculations if changes in primary beam intensity and beam quality. The largest difference in the isodose curves was found in buildup and the penumbra regions. **Conclusion:** The results showed that the dose calculation using Prowess TPS based on CCCS algorithm is generally in excellent agreement with measurements.

Keywords: Symmetric and Asymmetric Fields; Dose Calculation; Treatment Planning System

Introduction

The dose calculation algorithm must accurately model for all beam configurations normally used in the clinic. Radiation therapy treatment planning for many clinical situations requires asymmetric field size correctly modeled in the treatment planning computer system. This includes verifying the accuracy of both the isodose distributions and the monitor units (MUs) generated by the treatment planning system.[1-3] The degree of success achieved by the optimization process is largely dependent on the cost function used by the algorithm (which in turn depends on the structures defined by the user) and the algorithm used for minimization.[4] Several authors have conducted the evaluation of dose calculation algorithms for external beam radiation therapy.[5-7]

Commissioning of the dose calculation algorithms of a treatment planning system is generally performed: (i) by entering basic beam data into the system according to the methods and requirements described in the user's manual of the system; and (ii) by comparing the results of dose calculations with the entered data and with data that were measured specifically for this purpose. Most commonly, existing beam data are used as input data. Differences between calculated and actual dose values may be encountered, partly due to uncertainties in the measured data, and partly due to imperfect beam modeling. Criteria for acceptability have to be applied before accepting a treatment planning system for clinical use. Several authors have developed such criteria.[8] Several treatment planning systems calculate asymmetric fields on the assumption that these are equivalent to blocked fields. However, the parameters required for treatment planning implementation depend on the algorithm used, and the method of their derivation is often not explicit. Since asymmetric fields are the simplest case of irregular fields, others have approached this problem using appropriate algorithms that utilize the data available for symmetric fields.[9]

The collapse cone convolution algorithm is a point kernel convolution model that convolves a polyenergetic spectrum to the point kernel energy distribution and kernels correction during the convolution process is its main advantage.[10] Ahnesjö introduced CCC algorithm and for the first time, compared their dose calculation results with the Batho method A model may be capable to consider a given physical effect, but the actual implementation in the software is often simplified and can be resulted to inaccuracy or unexpected consequences. Thus many researches have verified the accuracy of the CCC algorithm against other dose calculation methods in different treatment planning systems (TPSs) and various clinical situations.[11] Prowess TPS has been available commercially for several years. As yet, however, there have been few reports [12, 13] studied the performance of Prowess TPS. The aim of our work is to determine the accuracy of

Corresponding author: Tamer Dawod; Department of Clinical Oncology and Nuclear Medicine, Faculty of Medicine, Mansoura University, Mansoura, Egypt.

***Cite this article as**: Dawod T. Evaluation of collapsed cone convolution superposition (CCCS) algorithms in prowess treatment planning system for calculat- ing symmetric and asymmetric field size. Int J Cancer Ther Oncol 2015; 3(2):3211. **DOI:** 10.14319/ijcto.32.11*

© Dawod

ISSN 2330-4049

Prowess TPS in dose calculation in a homogenous phantom for symmetric and asymmetric field size using collapse cone convolution/superposition algorithm.

Methods and Materials

The study was performed on a Siemens Artiste Linear Accelerator machine (Siemens Medical Solutions UK) for the 6 and 10 MV X-ray beam available at Alexandria Ayadi Al-Mostakbal Oncology Center. A computerized water tank system was used for dose measurements PTW dosimetry system (PTW, Freiburg, Germany) with two semiflex (0.125 cc) ionization chamber. The measurements were carried out at source-to-surface distance (SSD) set to 100 cm. Data for a full set of measurements for symmetric fields and asymmetric fields, including inplane and crossplane profiles at various depths and percentage depth doses (PDDs) were obtained during measurements on the linear accelerator. The position of the ionization chamber is critical in the case of asymmetric beams due to the dose gradient. The chamber was mounted in a holder, placed in a 50 cm × 50 cm × 50 cm PTW three dimensional water phantom. The gantry of the treatment unit was set to 0°. The linac was set to deliver 200 monitor units (MUs) per minute. To reduce the variability of working conditions, the dosimetry measurements were performed in a single session. The dose distributions were calculated by Prowess Panther version 5 (Prowess inc., Concord, CA) 3D planning system 3DTPS. The measured isodose was compared with the calculated isodose obtained from the Prowess TPSs under the same conditions as measured isodoses. The comparison made by using PTW VeriSoft software, Version 4 (PTW, Freiburg, Germany), and the reference isodose was the measured isodoses.

To verify agreement over the range of symmetric and asymmetric field sizes used clinically. Asymmetric fields obtained by shifting one or two of the collimator jaws across the collimator axis for the flowing field sizes 4 cm × 4 cm and 10 cm × 10cm. The different symmetric asymmetric field size was used in this study, for 4 cm × 4 cm and 10 cm × 10 cm showed in **Table 1**, **Figure 1** showed view of the beam setup at different depths of measurement (a) in the asymmetrical setting (X1 = 1, X2 = 3, Y1 = 2, Y2 = 2), (b) in the symmetrical setting (X1 = 2, X2 = 2, Y1 = 2, Y2 = 2), and (c) in the asymmetrical setting (X1 = 3, X2 = 1, Y1 = 2, Y2 = 2). Central axis depth dose and beam profiles measured at different depths (D_{max}, 5, 10, and 20 cm) and normalized to the value of d_{max} at the center. All data measured for inplane and crossplane direction at fixed SSD = 100 cm and for 6 and 10 MV for ARTISTE linac. Calculation was performed in a phantom created by the Prowess TPS used in this study with a homogeneous density of 1 g/cm^3, the dose grid used were 3 mm × 3 mm.

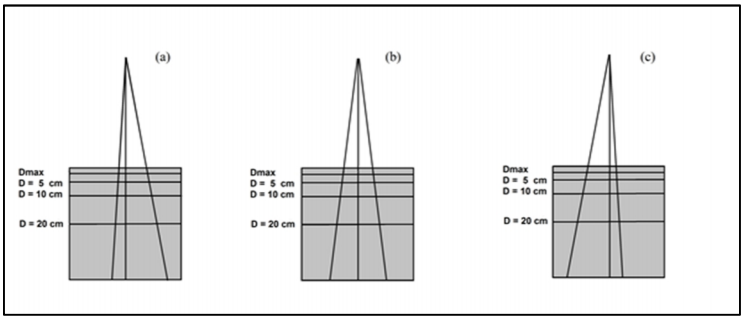

FIG. 1: View of the beam setup showing the depths of measurement (a) in the asymmetrical setting (X1 = 1, X2 = 3, Y1 = 2, Y2 = 2); (b) in the symmetrical setting (X1 = 2, X2 = 2, Y1 = 2, Y2 = 2); and (c) in the asymmetrical setting (X1 = 3, X2 = 1, Y1 = 2, Y2 = 2).

TABLE 1: Symmetric and asymmetric field sizes for crossplane and inplane direction.

No of Fields Examined	Crossplane Direction				Inplane Direction			
	X1	X2	Y1	Y2	X1	X2	Y1	Y2
	Field size (4 cm × 4 cm)							
1	1	3	2	2	2	2	1	3
2	2	2	2	2	2	2	2	2
3	3	1	2	2	2	2	3	1
	Field size (10 cm × 10 cm)							
1	2	8	5	5	5	5	2	8
2	3	7	5	5	5	5	3	7
3	4	6	5	5	5	5	4	6
4	5	5	5	5	5	5	5	5
5	6	4	5	5	5	5	6	4
6	7	3	5	5	5	5	7	3
7	8	2	5	5	5	5	8	2

© Dawod ISSN 2330-4049

Calculated dose validation

In order to compare calculated and measured doses, we used PTW VeriSoft software (Version 4) to verify the treatment plan by comparing calculated data to its corresponding measured in phantom.

According to the tolerance values for homogeneous simple fields, the penumbra region should be within 2 mm or 10%.[14-15] By just studying the profiles by eye it is hard to say, especially in the z-direction in the penumbra region, if the result is within the tolerance. A gamma evaluation with 3% and 3 mm criteria, revealing that it is only in the penumbra region that acceptance fails. The colors of the palette range are set to be green for 100% (γ = 1), and accepted regions are green and most yellow. Regions that fail are shown in red. The gamma evaluation method is not a good tool for evaluation of low dose regions, where the calculation can fail though it is within the set criteria. For example if we are comparing two dose points of 4% and 1% dose, and the dose criteria is set to be 2%, this will lead to a gamma value larger than 1 ((4%-1%)/2%). The 3% dose difference can still be within acceptable tolerances but the gamma calculation fails.

The acceptance criteria for evaluation between two plans using gamma index, varies from user to user. For example, some authors considered a dose difference criteria of ΔD = 5 %/5 mm and others as VanDyk *et al.* used 3%/3 mm. We used the VanDyk criteria in our analysis.[16] The criteria used is 3%-3 mm with the expectation that >90% of the points tested passing the 3%-3 mm criterion would be a minimum acceptable threshold.

The difference matrix of two detector array matrices is determined by comparison of the measured and the calculated asymmetric field sizes are expressed as a percentage of the locally measured dose by using the following equation:

$$\text{Diffrence (\%)} = (D_{calculated} - D_{measured})/D_{measured}) \times 100 \quad (1)$$

Results

The results of isodose curves for 6 and 10 MV and two opened field size 4 cm × 4 cm and 10 cm x 10 cm at 100 cm SSD were obtained. The measured isodose curves (measured by ionization chamber) compared with the calculated isodose curves (obtained from TPS) using γ-index evaluation for all asymmetric field sizes. **Figure 2 to 5** showed comparison of the dose distribution by the gamma method for both energies and different open asymmetric field size for Prowess treatment planning system. The results of the comparison were tabulated using the gamma method in **Table 2 and 3** for field size 4 cm × 4 cm, **Table 4** and **5** contains results for field size 10 cm × 10 cm.

Table 2 contained the percentage passing rate for the gamma index between measured and calculated symmetric and asymmetric field size obtained from field size 4 cm × 4 cm for both direction at 6 MV for Prowess treatment planning systems, it also contains the percentage failed rate between measured and calculated obtained from Prowess TPS. In crossplane direction the maximum difference was found at (X1 = 1, X2 = 3 & Y1 = 2, Y2 = 2), it equals to 5.5%. In inplane direction the maximum difference was found at (X1 = 2, X2 = 2 & Y1 = 1, Y2 = 3), it equals to 9%. The difference for most asymmetric fields was less than 5% except three points. **Figure 6** showed the difference between measured and calculated for crossplane and inplane at 6 MV. **Table 3** contains the percentage passing rate for the gamma index between measured and calculated symmetric and asymmetric field size obtained from field size 4cm × 4cm for both direction at 10 MV. In crossplane direction the maximum difference was found at (X1 = 1, X2 = 3 & Y1 = 2, Y2 = 2), it equals to 3.6%. In inplane direction the maximum difference was found at (X1 = 2, X2 = 2 & Y1 = 1, Y2 = 3), it equals to 4.5%. The difference for all asymmetric fields was less than 5%. **Figure 6** showed the difference between measured and calculated for crossplane and inplane at 10MV.

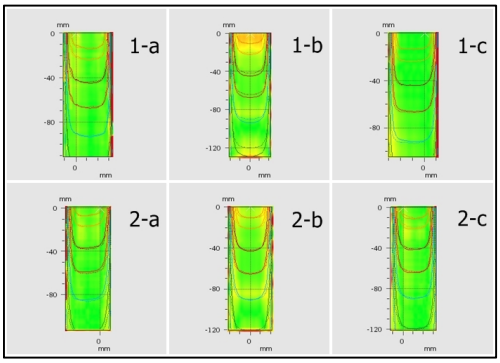

FIG. 2: Gamma distribution for different field using the full CCCS algorithm for 6 MV for field size 4 cm × 4 cm with different offsets. The upper parts represents the crossplane direction comparison, while the lower part represents the inplane direction comparison, the green color indicates regions where gamma ≤ 1; and red indicates gamma > 1 (individual criteria: Δ%D = 3%, DTA = 3 mm). For crossplane direction (a) (X1 = 1, X2 = 3, Y = 4); (b) (X1 = 2, X2 = 2, Y = 4); and (c) (X1 = 3, X2 = 1, Y = 4). For inplane direction (X = 4, Y1 = 1, Y2 = 3); (b) (X = 4, Y1 = 2, Y2 = 2); and (c) (X = 4, Y1 = 3, Y2 = 1).

TABLE 2: Difference between measured dose and calculated dose at different isodose lines for crossplane and inplane asymmetric fields for field size 4 cm × 4 cm at 6 MV.

GAMMA INDEX (3 mm)					
Crossplane Direction 6 MV					
Point No.	**Field Size(cm²)**	**Evaluated Dose Points**	**Passed Points**	**Failed Points**	**Matching Result**
1	(1,3)	100%	94.50%	5.50%	94.50%
2	(2,2)	100%	95.90%	4.10%	95.90%
3	(3,1)	100%	94.70%	5.30%	94.70%
Inplane Direction 6 MV					
1	(1,3)	100%	91.00%	9.00%	91.00%
2	(2,2)	100%	96.10%	3.90%	96.10%
3	(3,1)	100%	97.00%	3%	97.00%

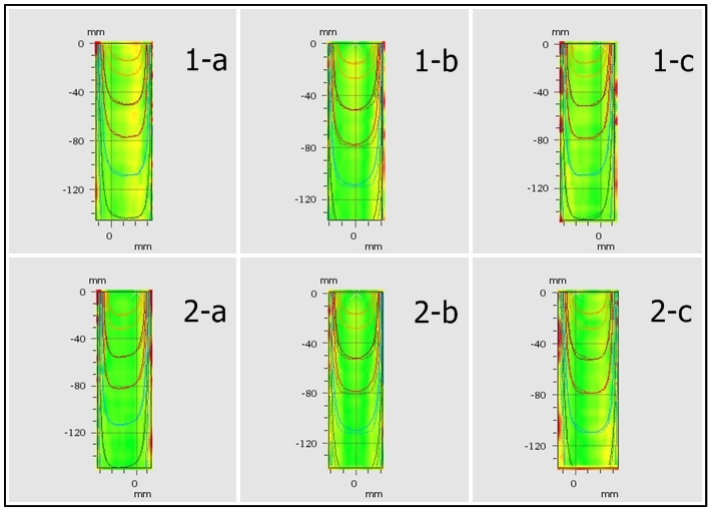

FIG. 3: Gamma distribution for different field using the full CCCS algorithm for 10 MV for field size 4 cm × 4 cm with different offsets.

TABLE 3: Difference between measured dose and calculated dose at different isodose lines for crossplane and inplane asymmetric fields for field size 4 cm × 4 cm at 10 MV.

GAMMA INDEX (3 mm)					
Crossplane Direction 10 MV					
Point No.	**Field Size(cm²)**	**Evaluated Dose Points**	**Passed Points**	**Failed Points**	**Matching Result**
1	(1,3)	100%	97.30%	2.70%	97.30%
2	(2,2)	100%	97.70%	2.30%	97.70%
3	(3,1)	100%	96.40%	3.60%	96.40%
Inplane Direction 10 MV					
1	(1,3)	100%	95.50%	4.50%	95.50%
2	(2,2)	100%	97.60%	2.40%	97.60%
3	(3,1)	100%	97.00%	3%	97.00%

© Dawod

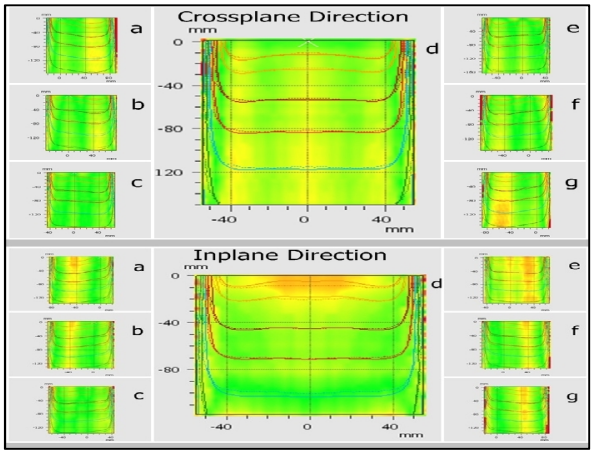

FIG. 4: Gamma distribution for different field using the CCCS algorithm for 6 MV for field size 10 cm × 10 cm with different offsets. The upper parts represent the crossplane direction comparison, while the lower part represents the inplane direction comparison.

TABLE 4: Difference between measured dose and calculated dose at different isodose lines for crossplane and inplane asymmetric fields for field size 10 cm × 10 cm at 6 MV.

GAMMA INDEX (3mm)					
Crossplane Direction 6 MV					
Point No.	**Field Size(cm^2)**	**Evaluated Dose Points**	**Passed Points**	**Failed Points**	**Matching Result**
1	(2,8)	100%	97.60%	2.40%	97.60%
2	(3,7)	100%	97.90%	2.10%	97.90%
3	(4,6)	100%	98.10%	1.90%	98.10%
4	(5,5)	100%	98.70%	1.30%	98.70%
5	(6,4)	100%	98.60%	1.40%	98.60%
6	(7,3)	100%	98.50%	1.50%	98.50%
7	(8,2)	100%	98.00%	2%	98.00%
Inplane Direction 6 MV					
Point No.	**Field Size(cm^2)**	**Evaluated Dose Points**	**Passed Points**	**Failed Points**	**Matching Result**
1	(2,8)	100%	99.00%	1.00%	99.00%
2	(3,7)	100%	98.20%	1.80%	98.20%
3	(4,6)	100%	98.60%	1.40%	98.60%
4	(5,5)	100%	99.10%	0.90%	99.10%
5	(6,4)	100%	98.70%	1.30%	98.70%
6	(7,3)	100%	98.00%	2.00%	98.00%
7	(8,2)	100%	96.70%	3%	96.70%

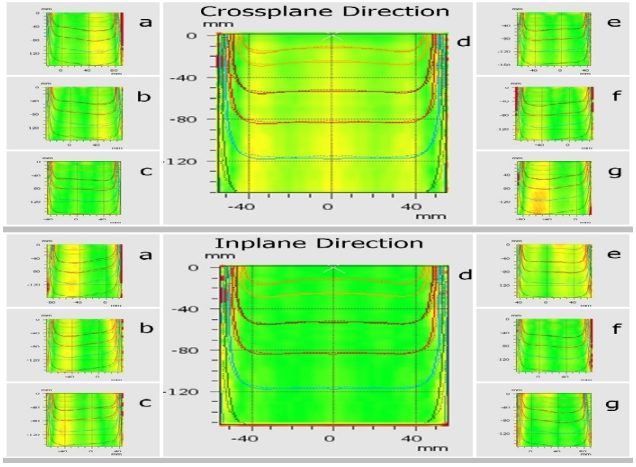

FIG. 5: Gamma distribution for different field using the CCCS algorithm for 10 MV for field size 10 cm × 10 cm with different offsets. The upper parts represent the crossplane direction comparison, while the lower part represents the inplane direction comparison.

TABLE 5: Difference between measured dose and calculated dose at different isodose lines for crossplane and inplane asymmetric fields for field size 10 cm × 10 cm at 10 MV.

GAMMA INDEX (3mm)					
Crossplane Direction 10MV					
Point No.	**Field Size(cm^2)**	**Evaluated Dose Points**	**Passed Points**	**Failed Points**	**Matching Result**
1	(2,8)	100%	97.30%	2.70%	97.30%
2	(3,7)	100%	99.50%	0.50%	99.50%
3	(4,6)	100%	99.20%	0.80%	99.20%
4	(5,5)	100%	99.30%	0.70%	99.30%
5	(6,4)	100%	99.00%	1.00%	99.00%
6	(7,3)	100%	97.40%	2.60%	97.40%
7	(8,2)	100%	98.70%	1%	98.70%
Inplane Direction 10MV					
Point No.	**Field Size(cm^2)**	**Evaluated Dose Points**	**Passed Points**	**Failed Points**	**Matching Result**
1	(2,8)	100%	96.50%	3.50%	96.50%
2	(3,7)	100%	98.00%	2.00%	98.00%
3	(4,6)	100%	98.20%	1.80%	98.20%
4	(5,5)	100%	99.00%	1.00%	99.00%
5	(6,4)	100%	98.80%	1.20%	98.80%
6	(7,3)	100%	96.60%	3.40%	96.60%
7	(8,2)	100%	98.40%	1.60%	98.40%

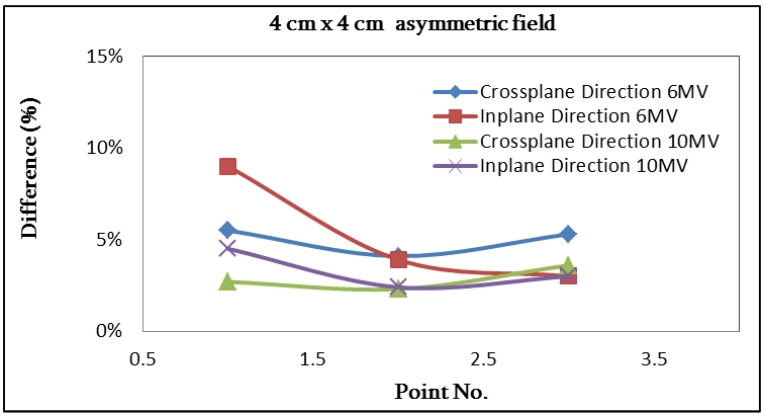

FIG. 6: Comparison between crossplane and inplane difference for 4 cm × 4 cm with different offsets for 6 MV and 10 MV.

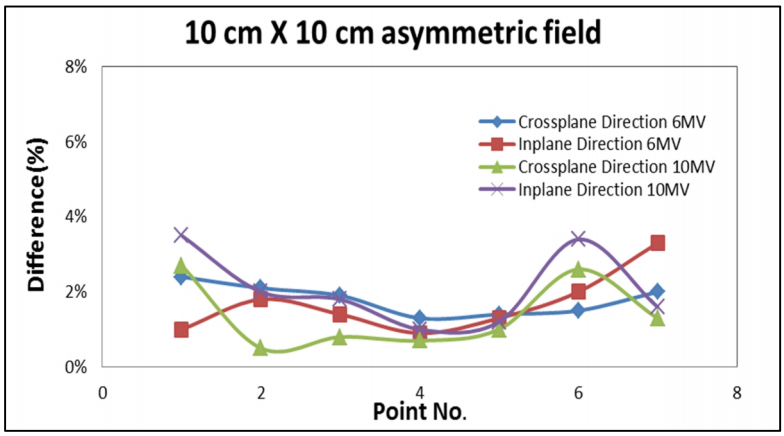

FIG. 7: Comparison between crossplane and inplane difference for 10 cm × 10 cm with different offsets for 6 MV and 10 MV.

Table 4 presents the percentage passing rate for the gamma index between measured and calculated symmetric and asymmetric field size obtained from field size 10 cm × 10 cm for both direction at 6 MV. In crossplane direction the maximum difference was found at (X1 = 2, X2 = 8 & Y1 = 5, Y2 = 5), it equals to 2.4% TPS. In inplane direction the maximum difference was found at (X1 = 5, X2 = 5 & Y1 = 8, Y2 = 2), it equals to 3%. The difference for all asymmetric fields was less than or equal to 3%, and the uncertainty limitation of this work equals to ±3%. **Figure 7** Showed the difference between crossplane and inplane for 10MV. **Table 5** percentage passing rate for the gamma index between measured and calculated symmetric and asymmetric field size obtained from field size 10 cm × 10 cm for both directions at 10MV. In crossplane direction the maximum difference was found at (X1 = 2, X2 = 8 &Y1 = 5, Y2 = 5), it equals to 2.7%. In inplane direction the maximum difference was found at (X1 = 5, X2 = 5 & Y1 = 2, Y2 = 8), it equals to 3.5%. The difference for all asymmetric fields was less than 3% except two points. **Figure 7** showed the difference between measured and calculated for crossplane and inplane at 10 MV.

Discussion

Quality assurance of treatment planning systems has been the subject of study of several groups of physicists, formulating recommendations for the commissioning and routine quality control of these systems.[8] Different types of studies can be distinguished. Sauer *et al.*[17] presented studies, in which the performance of one specific treatment planning system was discussed, using machine data obtained in the same clinic and comparing these data with results of calculations. The asymmetric fields is smaller than the symmetric field in one dimension, this reduction leads to decrease in the absorbed dose in this direction which made significant alteration in the depth dose and beam profile.The beam profile and isodose lines for the asymmetric field differ than the symmetric field with the same field size; this difference is due to that the asymmetric field intercepts different positions in the flatting filter which leads to decrease in scattered radiation in one side than the other side. This effect leads to tilt in one side (wedge effect) of the beam profile and isodose lines.

In this study, dose calculation accuracy of CCCS has been evaluated by comparing the measured and calculated isodose lines in homogeneous water phantom. The data showed that the difference in the small asymmetric fields higher than the larger asymmetric fields. The average difference between measured and calculated field size 4 cm × 4 cm with different offsets is 4.11 ± 0.02, while for field size 10 cm × 10 cm with different offsets is 1.73 ± 0.008 for Prowess TPS. The comparison between measured and calculated dose made by gamma index method showed that the average difference for asymmetric fields is less than 3%. Except for field size 4 cm × 4 cm, our data compared with previous data from Birgani *et al.*[18], El-Attar *et al.*[9], Chegeni and Birgani[19, 20], and Murugan *et al.*[21] Asymmetric collimation dose lead to significant errors (up to approximately 7%) in dose calculations if changes in primary beam intensity and beam quality.[22] It is obvious that the most difference in the isodose curves was found in buildup region and the penumbra region. Constrictions of isodose curves at the edge nearer to central axis for asymmetrically placed fields are obvious. This is attributed to the decrease of primary and side scattered radiation caused by geometrical non-divergence of the beam at that edge which leads to wedge shape, this agreed with C. Varatharaj *et al.*[23] The agreement between measured and calculated isodoses is better for 10 MV than for 6 MV, where the highest difference equal to 2% was observed when both the crossplane and inplane directions are moved to their mechanical limit for over travel. The results showed that most data gave a high passing rate (>97%) for the gamma index for Prowess TPS approved the suitability of CCCS algorithm for incorporation into a treatment planning system for asymmetric opened fields. The methodology applied in this study can also be implemented to validate other advanced dose calculation algorithms such as Acuros XB algorithm and anisotropic analytical algorithm.[25-27]

Conclusion

Dose calculation using Prowess TPS based on CCCS algorithm is generally in excellent agreement with measurements. There are some points with deviation which was not within the limits that have been set up for dose planning systems; the largest deviation was found at the small field size 4 cm × 4 cm. The reason of that deviation is the uncertainty in dose measurement in addition to the tilt effect. Based on our results, the Prowess Panther v5.01 Planning System and CCCS algorithm, were within the acceptable accuracy limits in dosimetry. The additional dosimetry should be done in the region above the depth of maximum dose using a proper dosimeter.

Conflict of interest

The authors declare that they have no conflicts of interest. The authors alone are responsible for the content and writing of the paper.

References

1. Alaei P, Higgins PD, Gerbi BJ. Implementation of enhanced dynamic wedges in Pinnacle treatment planning system. *Med Dosim* 2005; **30**:228-32.
2. Jacques R, Taylor R, Wong J, McNutt T. Towards real-time radiation therapy: GPU accelerated superposition/convolution. *Comput Methods Programs Biomed* 2010; **98**:285-92.

3. Sutter H. The free lunch is over: a fundamental turn toward concurrency in Software. *Dr. Dobb's J* 2005, **30**.
4. Petric MP, Clark BG, Robar JL. A comparison of two commercial treatment-planning systems to IMRT. *J Appl Clin Med Phys* 2005; **6**:63-80.
5. Oyewale S. Dose prediction accuracy of collapsed cone convolution superposition algorithm in a multi-layer inhomogenous phantom. *Int J Cancer Ther Oncol* 2013; **1**:01016.
6. Das IJ, Ding GX, Ahnesjö A. Small fields: nonequilibrium radiation dosimetry. *Med Phys* 2008; **35**:206-15.
7. McNutt T. Dose calculations: collapsed cone convolution superposition and delta pixel beam. 2002: Pinnacle White Paper No. 4535 983 02474.
8. Venselaar J, Welleweerd H. Application of a test package in an intercomparison of the photon dose calculation performance of treatment planning systems used in a clinical setting. *Radiotherapy and Oncology* 2001; **60**:203-13.
9. El-Attar AL, Abdel-Wanees ME, Hashem MA. Dose measurement and calculation of asymmetric x-ray fields from therapeutic linac. *Tenth Radiation Physics & Protection Conference*, Egypt, 2010.
10. Ahnesjö A. Collapsed cone convolution of radiant energy for photon dose calculation in heterogeneous media. *Med Phys* 1989; **16**:577-92.
11. Moradi F, Mahdavi SR, Mostaar A, Motamedi M. Commissioning and initial acceptance tests for a commercial convolution dose calculation algorithm for radiotherapy treatment planning in comparison with Monte Carlo simulation and measurement. *J Med Phys* 2012; **37**:145-50.
12. Ayşegül ÜK, Özgehan O, Songül K, *et al*. Dosimetric verification of prowess panter treatment planning system and the evaluation of the clinical acceptance. *Turkish Journal of Oncology* 2012; **27**:76-82.
13. Eldesoky I, Attalla EM, Elshemey WM, Zaghloul MS. A comparison of three commercial IMRT treatment planning systems for selected paediatric cases. *J Appl Clin Med Phys* 2012; **13**:3742.
14. Zhen H, Nelms BE, Tome WA. Moving from gamma passing rates to patient DVH-based QA metrics in pretreatment dose QA. *Med Phys* 2011; **38**:5477-89.
15. Venselaar J, Welleweerd H, Mijnheer B. Tolerances for the accuracy of photon beam dose calculations of treatment planning systems. *Radiother Oncol* 2001; **60**:191-201.
16. Van Dyk J, Barnett RB, Cygler JE, Shragge PC. Commissioning and quality assurance of treatment planning computers. *Int J Radiat Oncol Biol Phys* 1993; **26**:261-73.
17. Sauer O, Nowak G, Richter J. Accuracy of dose calculations of the Philips treatment planning system OSS for blocked fields. Quality assurance in treatment planning. Report from the German task group Proc. Xth ICCR. In: Bruinvis IAD, van der Giessen PH, van Kleffens HJ, Whitkamper FW, editors. The use of computers in radiation therapy. Amsterdam, Elsevier, 1987.
18. Tahmasebi Birgani MJ, Chegeni N, Zabihzadeh M, Hamzian N. An analytical method to calculate equivalent fields to irregular symmetric and asymmetric photon fields. *Med Dosim* 2014; **39**:54-9.
19. Chegeni N, Tahmasebi Birgani M J. Equivalent field calculation to irregular symmetric and asymmetric photon fields. *International Journal of Medical, Health, Pharmaceutical and Biomedical Engineering* 2013; **7**.
20. Chegeni N, Tahmasebi Birgani MJ. Profile calculation in water phantom of symmetric and asymmetric photon beam. *World Academy of Science, Engineering and Technology. International Journal of Mathematical, Computational, Physical and Quantum Engineering* 2013; 7.
21. Murugan A, Valas XS, Thayalan K, Ramasubramanian V. Dosimetric evaluation of a three-dimensional treatment planning system. *J Med Phys* 2011; **36**:15-21.
22. Salk JE. A simple formalism for calculation and verification of dose in asymmetric x-ray fields. Department of Radiotherapy, University of Ulm, D-89081 Ulm, Germany.
23. Varatharaj C, Ravikumar M, Supe SS, *et al*. Dosimetric investigation of dual energy photon beams with assymmetric collimator jaws. *Pol J Med Phys Eng* 2008; **14**:33-45.
24. Hilton J. Capacity-Building for the radiation protection dividend: A twelve point blueprint for strengthening and sustaining the professional radiation protection community in Africa, A Consultation Paper, Nairobi, September 15, 2010.
25. Rana S, Rogers K, Lee T, Reed D, Biggs C. Dosimetric impact of Acuros XB dose calculation algorithm in prostate cancer treatment using RapidArc. *J Cancer Res Ther* 2013; **9:430**-5.
26. Ojala J. The accuracy of the Acuros XB algorithm in external beam radiotherapy – a comprehensive review. *Int J Cancer Ther Oncol* 2014; **2**:020417.
27. Lu L. Dose calculation algorithms in external beam photon radiation therapy. *Int J Cancer Ther Oncol* 2013; **1**:01025.

© Dawod ISSN 2330-4049